JCTC Journal of Chemical Theory and Computation

Article

pubs.acs.org/JCTC

Insight into the Properties of Cardiolipin Containing Bilayers from Molecular Dynamics Simulations, Using a Hybrid All-Atom/United-Atom Force Field

Daniel Aguayo,[†,‡,§] Fernando D. González-Nilo,[‡,§] and Christophe Chipot*[,∥,⊥]

[†]Centro de Bioinformática y Simulación Molecular, Facultad de Ingeniería en Bioinformática, Universidad de Talca, 2 Norte 685, Casilla 721, Talca, Chile

[‡]Centro de Bioinformática y Biología Integrativa, Facultad de Ciencias Biológicas, Universidad Andrés Bello, República 239, Santiago, Chile

[§]Centro Interdisciplinario de Neurociencia de Valparaíso, Universidad de Valparaíso, Valparaíso, Chile

[∥]Theoretical and Computational Biophysics Group, Beckman Institute for Advanced Science and Engineering, University of Illinois at Urbana−Champaign, 405 North Mathews, Urbana, Illinois 61801, United States

[⊥]Équipe de dynamique des assemblages membranaires, UMR 7565, Université de Lorraine, BP 239, 54506 Vandoeuvre-lès-Nancy cedex, France

Supporting Information

ABSTRACT: Simulation of three models of cardiolipin (CL) containing membranes using a new set of parameters for tetramyristoyl and tetraoleoyl CLs has been developed in the framework of the united-atom CHARMM27-UA and the all-atom CHARMM36 force fields with the aim of performing molecular dynamics (MD) simulations of cardiolipin-containing mixed-lipid membranes. The new parameters use a hybrid representation of all-atom head groups in conjunction with implicit-hydrogen united-atom (UA) to describe the oleoyl and myristoyl chains of the CLs, in lieu of the fully atomistic description, thereby allowing longer simulations to be undertaken. The physicochemical properties of the bilayers were determined and compared with previously reported data. Furthermore, using tetramyristoyl CL mixed with POPG and POPE lipids, a mitochondrial membrane was simulated. The results presented here show the different behavior of the bilayers as a result of the lipid composition, where the length of the acyl chain and the conformation of the headgroup can be associated with the mitochondrial membrane properties. The new hybrid CL parameters prove to be well suited for the simulation of the molecular structure of CL-containing bilayers and can be extended to other lipid bilayers composed of CLs with different acyl chains or alternate head groups.

1. INTRODUCTION

Mitochondria are organelles that provide most of the chemical energy required by the cell, namely adenosine triphosphate (ATP), from oxidative metabolism. In the inner mitochondrial membrane (IMM) is found an unusual type of dimeric phospholipid, cardiolipin (CL), the structure of which consists of three glycerol backbones, four acyl chains and a divalent anionic headgroup (see Figure 1).[1] CLs play multiple roles related to energy transformation, apoptosis and membrane integrity.[2,3] Several mitochondrial proteins have been shown to require CLs for their optimal activity. Such is the case, among others, of cytochrome P-450$_{SCC}$,[4] mitochondrial creatine kinase,[5,6] mitochondrial L-glycerol-3-phosphate dehydrogenase[7] and mitochondrial carnitine acylcarnitine translocase.[8] A number of investigations have suggested that CLs are associated with the mitochondrial apoptotic pathway,[9] or different complexes of the respiratory chain, involved in the transduction of electrons and the synthesis of ATP in the IMM.[10,11] In addition, CLs are of paramount importance in the formation of contact sites between the inner and outer mitochondrial membrane by virtue of its ability to arrange spatially into hexagonal H_{II} phases.[12] They are also related to membrane lipid polarization in prokaryotic organisms in a process mediated by CL intrinsic curvature.[13,14]

Detailed structural information of CLs is admittedly scarce: only a handful of data on CL aggregates and IMM protein−CL interactions have been reported hitherto.[15] A number of structures deposited in the Protein Data Bank (PDB) contain CLs cocrystallized with IMM proteins.[16−19] Because CLs were cocrystallized with the protein, the conformation of these lipids is not necessarily representative of that found in a hydrated bilayer.

Computer simulations have proven to constitute a useful approach to study the properties of lipid aggregates.[20,21] Simulations can be employed to investigate the dynamics of individual molecules and the assembly thereof, with the potential to attain a much more detailed picture than would be obtained at the experimental level. Moreover, computer simulations allow theoretical and experimental parameters to be compared directly and are now sufficiently reliable to endeavor the investigation of molecular assemblies that can only be

Received: November 23, 2011
Published: April 16, 2012

   dx.doi.org/10.1021/ct200849k | J. Chem. Theory Comput. 2012, 8, 1765−1773

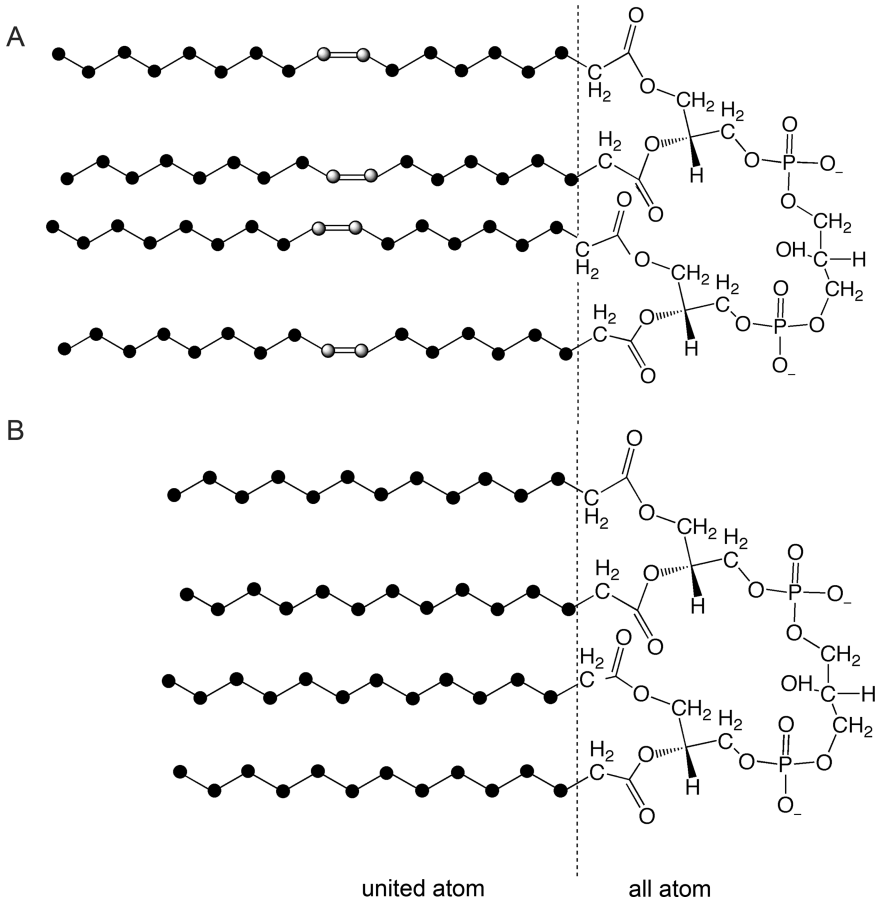

Figure 1. Hybrid force field assignment and molecular structure of cardiolipins. Tetraoleoyl (A) and Tetramyristoyl (B) used in this work. The type and net atomic charges borne by the different atoms can be found in the Supporting Information.

tackled experimentally at the price of significant technical difficulties. These observations in conjunction with the dearth of experimental results have motivated the simulation of CL phases. Dahlberg et al. applied MD simulations to a set of coarse-grained models of CL derivatives,[22] wherein the number of acyl-chain tails were varied alongside with the pH to induce phase transitions between micellar, lamellar, and inverted hexagonal phases. More recently, the same group simulated bilayers formed by CLs only, as well as by mixtures of CLs and phosphatidylcholine lipids.[23] In the latter work, the authors employed a lipid interaction model based on the original, united-atom force field of Berger et al.[24] Róg et al.[25] studied the role of CLs in a mixture of phospholipids using the OPLS force field, and observed a different behavior of the membrane phases as a function of the membrane composition.

One of the problems deeply rooted in the molecular simulations of biological membranes is the simulation time required to model lipid aggregation and, more generally, self-diffusion. Simulation of large systems covering long time scales, usually require the use of models with a reduced atomic definition (i.e., united-atom, coarse-grained descriptions) for the sake of sampling, but at the expense of accuracy on the atomic-level interactions. Moreover, simulations that bring to light the atomic detail of intermolecular interactions, for example, hydrogen bonding, between head groups, ions binding are by and large limited to assays of small size and short time scales. This intrinsic limitation can be circumvented by combining united- and all-atom descriptions, which guarantees energetic accuracy, while constituting a computationally efficient strategy.

In the present contribution, use is made of the update of the additive all-atom CHARMM lipid force field (c36) introduced by Klauda and collaborators[26,27] for head groups and the united-atom representation of the acyl chains in phospholipids (c27-UA) developed recently by Hénin et al.[28] The new sets of parameters proposed herein (see Supporting Information) were utilized to study pure and mixed bilayers containing CLs of different acyl-chain lengths, with the objective to model mitochondrial membranes.

2. MATERIALS AND METHODS

2.1. Molecular Assemblies. In the absence of a structure of an isolated tetraoleoyl-cardiolipin (TOCL), the latter was constructed from the cocrystallized CLs found in the 1QOV entry of PDB (http://www.rcsb.org). This structure was modified using the Hyperchem software,[29] namely, all the acyl chains were transformed into oleoyl chains, and its geometry was subsequently optimized quantum-mechanically at the semiempirical, AM1 level.[30] Hydrogen atoms of the oleoyl chains were then eliminated to generate the connectivity list and the initial Cartesian coordinates. The hybrid c36-UA topology for CLs, featuring the net atomic charges, is based on a combination of the recently developed c36 force field for the headgroup,[26] and the c27-UA parametrization for lipids tails.[28] To create a library of lipid configurations, the TOCL unit was replicated, using the VMD visualization program,[31] into a regular array in the *x,y*-plane of the bilayer from whence a

Table 1. Structural Properties of the Simulated Pure Cardiolipin Bilayer[a]

name	number of lipids	Na^+ per lipid	water per lipid	simulated time [ns]	$\langle A_L \rangle$ [nm^2]	thickness [nm]	K_A [dyn/cm]
128TOCL	128 TOCL	2	198	160	1.24 ± 0.1	4.2 ± 0.3	436.7
128TMCL	128 TMCL	2	198	160	1.03 ± 0.2	3.7 ± 0.1	424.1

[a]Average area per lipid ($\langle A_L \rangle$) and compressibility modulus (K_A), and bilayer thickness calculated as the distance between phosphate groups in adjacent leaflets of the bilayer.

membrane patch of 16 lipids per leaflet was created. This membrane patch was hydrated and equilibrated for 1 ns. TOCL lipids were then extracted randomly from the trajectory. With this library, a new TOCL patch was generated containing 16 lipids per leaflet (16 TOCL), hydrated, energy-minimized for 5000 steps and subsequently equilibrated for 2 ns. From the 16 TOCL patch, a new bilayer featuring 64 TOCLs per leaflet was assembled, that is, altogether 128 TOCLs. A 5-nm slab of water was added on each side of the bilayer, and the system was neutralized by means of sodium counterions, using VMD. The complete molecular assembly consisted of 91,244 atoms and its initial dimensions were 9.6 × 9.6 × 1.40 nm^3. The tetramyristoyl-cardiolipin (TMCL) bilayer was constructed from an equilibrated 128 TOCL bilayer, transforming the oleoyl chains into myristoyl chains. To model the IMM, a mixed bilayer membrane was constructed, using two different lipid arrays of 48 POPE, 16 POPG (8 L- and 8 D-POPG lipids) and 8 TMCL. Each lipid was positioned with a visual inspection to ensure a homogeneous distribution of TMCL and POPG units. The obtained bilayer was hydrated with a 5-nm slab of water and neutralized by means of sodium counterions. The CL-containing mixed lipid bilayer consisted of 75 766 atoms and its initial dimensions were 10 × 10 × 10.40 nm^3.

2.2. Molecular Dynamics Simulations. All MD simulations were performed with the software NAMD 2.8.[32] The hydrated membrane formed by 128 TOCLs (128TOCL), 128 TMCLs (128TMCL), and mixed lipids (MIX) were first energy-minimized for 5,000 steps and equilibrated for 1 ns at constant volume and 400 K (NVT), with the lipid tails free to move. The systems were then equilibrated at constant pressure and temperature (NPT). During the first 2 ns of equilibration, the water molecules were restrained to be outside the bilayer core to enhance acyl chain packing. The 128TOCL, 128TMCL, and MIX systems were then equilibrated, bereft of any geometrical restraints, for a period of 40 ns prior to the production simulation, which lasted ∼160 ns per system. The MD simulations were carried out with a time step of 2 fs and a 12-Å spherical cutoff for short-range nonbonded interactions, including a switching function from 10 Å for the van der Waals term and shifted electrostatics. For long-range, electrostatic interactions, the particle-mesh Ewald (PME) method was utilized with a grid spacing on the order of 1 Å or less. The simulations were performed at a temperature of 310 K, in the NPT ensemble, with fully anisotropic pressure coupling, in absent of additional surface tension component, which is obviated by the use of the c36 force field for the headgroup.[26] The Langevin piston method[33] was used to control the pressure. The temperature was maintained constant by means of Langevin dynamics with a damping coefficient of 1 ps^{-1}. Periodic boundary conditions were applied to all simulations. The equations of motion were integrated with the resp-A multiple time-step algorithm,[34] with an effective time step of 2, 2, and 4 fs for bonded, short- and long-range nonbonded interactions, respectively. The TIP3P model of water was used.[35] All the simulations made use of new parameters for TMCL and TOCL derived from additions and modifications of CHARMM 27 (c27),[36] the c36,[26] and the c27-UA[28] force fields.

2.3. Electrostatics Calculations. The electrostatic potential of the complete molecular assemblies was mapped using the PMEPOT plugin of VMD[37] with a grid spacing of less than 1 Å. Three-dimensional evaluation of the electrostatic potential was performed over the complete production simulations, that is, 160 ns. The quantity reported herein corresponds to an average over this period of time. The midplane of the bilayer was considered to be at 0 V.

2.4. Area per Lipid and Membrane Thickness. To calculate the area per lipid of pure bilayers, the total x,y−area of the lipid box was divided by the number of lipids present on each leaflet of the membrane and averaged over the trajectory. A Voronoi tessellation analysis[38] was performed for the trajectory of the mixed lipid bilayer. A Voronoi grid was constructed with the coordinates of the center of mass of each lipid, considering the nearest periodic images to eliminate cells with infinite area. The analysis was used to calculate the average area for each lipid and its relationship with the total area of the bilayers. The membrane thickness for 128TMCL and 128TOCL pure bilayers was calculated using the phosphorus-to-phosphorus distance from the probability density calculations. For the MIX bilayer, the thickness was calculated as the distance projected along the z-direction between phosphorus atoms pertaining to each membrane leaflet, using a sliding square window of 0.25 nm^2.

3. RESULTS AND DISCUSSION

One of the many problems associated to the molecular simulations of membrane systems is the computational cost required to sample properly. At the same time, when experimental data is scarce, as is the case for CL bilayers, simulation of lipid membrane systems raises difficulties, because the lateral force needed to describe accurately the mechanical properties of the system cannot be determined unambiguously.[39] The reduced c27-UA[28] united-atom parameter set for acyl chains has been successfully used to simulate lipid bilayers composed of lipids smaller than CLs, with both accuracy and reduced computational cost. c27-UA was designed within the framework of the c27 force field for lipids, for which the use of a constant surface area or a constant surface tension ensemble is suggested.[40] To circumvent this methodological issue, use was made of the headgroup parameters of the additive all-atom c36[26] lipid force field. This force field has been probed to represent properties, such are the area per lipid and order parameters of different lipid bilayers without application of additional lateral external forces, yielding structural properties that are in good agreement with experimental data.[27] In this work, a new set of parameters for TOCL and TMCL based on a hybrid all atom c36/united atoms c27-UA combination is proposed. In the following sections, this combination is used to describe the structure and dynamics of CL-containing bilayers

in terms of their area per lipid, order parameters, thickness, and electrostatic potential.

3.1. Pure TMCL and TOCL Cardiolipin Bilayers.

3.1.1. Membrane Characterization. The average of the area per lipid unit, $\langle A_L \rangle$, was calculated to describe the bilayer microstructure from the perspective of molecular packing. In addition, the compactness of the bilayer was estimated from an analysis of the surface area per lipid, the width and the compressibility. The area per lipid, $\langle A_L \rangle$, and the compressibility modulus, K_A, are gathered in Table 1.

The area per lipid for the 128TOCL bilayer was found to be equal to 1.24 nm^2. The A_L for the TOCL has not been determined experimentally, but an estimate of 1.2 nm^2 has been put forth by Goormaghtigh and co-workers based on the bilayer surface charge.[41,42] Aside from differences in the head groups, it is noteworthy that the area per acyl chain for the 128TMCL cardiolipin bilayer (~0.25 nm^2) is remarkably low compared to that of POPE or POPC (~0.30 nm^2), which are both zwitterionic phospholipids. This quantity is, however, comparable to the area of the closely related anionic lipid POPG, namely, 0.265 nm^2 per acyl chain.[43] A reduced area per lipid has been reported on similar anionic lipids,[43−45] thereby supporting the present results.

The thickness of the bilayer was found to be equal to about 3.7 and 4.2 nm for 128TMCL and 128TOCL, respectively (see Table 1), calculated as the distance between phosphate groups pertaining to adjacent leaflets. The distributions of phosphorus atoms, water, and sodium ions along the normal to the interface, that is, the z-direction of Cartesian space, are shown in Figure 2. As expected, the 128TOCL is thicker than

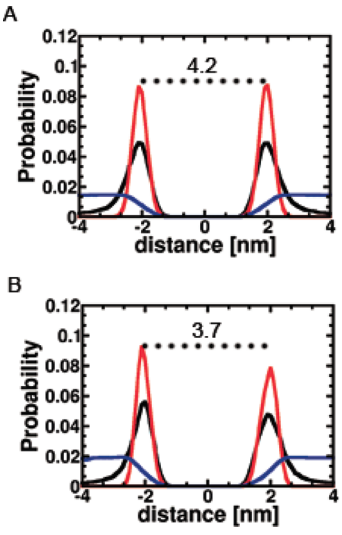

Figure 2. Characteristic features of the TMCL (A) and TOCL (B) bilayers. The probability density of water (blue), sodium (black) and phosphorus (red) atoms of CLs are shown as a function of their distance from the center of the bilayer. Averaging was performed over 160 ns of production MD trajectory.

128TMCL bilayer, which is in part rationalized by the increased fraction of carbon in the oleoyl chains of TOCL, compared to the myristoyl chains of TMCL.

To determine if the order of the acyl chains contribute to the differences observed on the thickness and A_L, the profile of local order parameter, S_{CD}, was calculated and reported in Figure 3. The order parameter for the n^{th} segment of an acyl chain was calculated using:

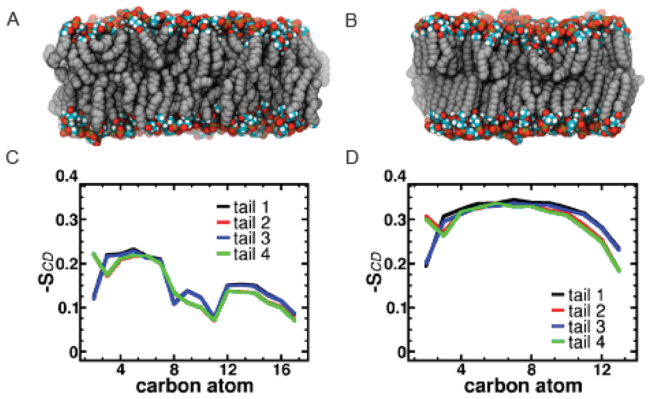

Figure 3. Representative configuration of the pure bilayers and local order parameter (S_{CD}) of the four acyl chains of TOCLs (A,C) and TMCLs (B,D). Averaging was performed over 160 ns of production MD trajectory.

$$|S_{CD}| = \frac{1}{2}\langle 3\cos^2\theta - 1\rangle \quad (1)$$

where θ is the instantaneous angle between the nth segment vector, that is, the (C_{n-1}, C_{n+1}) vector linking the $n-1$th and the $n+1$th carbon atoms in the acyl chain and the normal to the plane of the bilayer; $\langle ... \rangle$ denotes both ensemble and time averages. The S_{CD} profile are in overall agreement with other simulations performed with other force-field parameters for TOCL.[25] When compared with the results for the sn-2 chain of POPC,[28] DPPC,[46] and POPG,[45] the overall behavior for CLs appears to be similar, although the order is slightly more pronounced for the CL chains near the headgroup. When compared with TOCL, TMCL has a more ordered profile, a result in agreement with other simulations using a different force field.[45,46] Put together, it may be inferred that TMCLs are by and large more ordered near the headgroup region and acyl chains, while TOCLs, with their disordered acyl chains on account of kinks from the cis bonds, induce disorder of the membrane in the hydrophobic core. According to the experimental results from Lewis et al., the A_L values presented herein correspond to a TMCL membrane in the L_α phase.[48] Whereas the A_L is in agreement with the work of Dahlberg and Maliniak,[23] there is some discrepancy in the S_{CD} profiles, where our estimate indicates a reduced order of the bilayer, compared to the aforementioned work, which corresponds to a L_β phase. Taking into account the chosen simulation temperature of 37 °C, close to the L_α/L_β transition temperature occurring experimentally at 40 °C for TMCLs,[48] the calculated A_L and the S_{CD} profiles presented reflect an intermediate regime between the L_α and L_β phases. To clarify this observation and improve the proposed parameters, multiple simulations ought to be performed below, above and at the L_α/L_β phase transition temperature, where the reduced computational cost of the proposed hybrid all atoms/united atoms CL parameters are envisioned to be useful. Such a clarification goes beyond the scope of the present work.

From the total area and its fluctuations, the area compressibility modulus (K_A) is defined by

$$K_A = \frac{k_B T\langle A\rangle}{N\langle (A - A_0)^2\rangle} \quad (2)$$

where k_B is the Boltzmann constant, T, the temperature, N, the number of lipids per leaflet, and A_0, the equilibrium area per

lipid.[49] For the present 128TOCL and 128TMCL bilayers, K_A was found to amount to about 437 and 424 mN/m. This value is noteworthily different from the values reported previously by Dahlberg and Maliniak for TOCL, using a smaller assay.[23] This difference can be rationalized by the effect of the acyl-chain order on the membrane elastic properties: the bilayers described here, as mentioned previously, have a reduced acyl order than that reported by Dahlberg and Maliniak.[23] It is, however, noteworthy that this elastic property, as well as others like the membrane curvature, requires for its convergence large membrane patches and long simulation times to take into account the undulations of the bilayer and the variations of the area per leaflet.

3.1.2. Intramolecular Hydrogen Bond and Headgroup Geometry. The calculated intramolecular distances between the central hydroxyl and the phosphate oxygen atoms are shown in Figure 4. For the 128TOCL and 128TMCL bilayers, the first

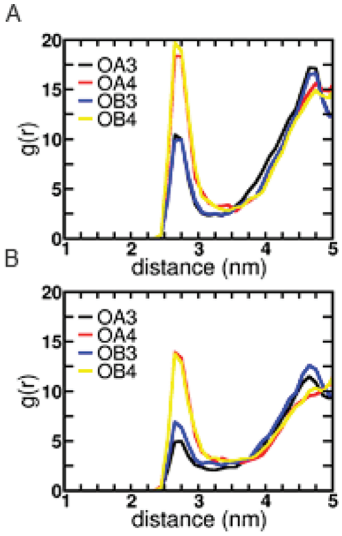

Figure 4. Intramolecular hydrogen bonds calculated using the pair correlation function between hydroxyl and phosphate oxygens for (A) 128TOCL, (B) 128TMCL, and (C) MIX. Headgroup naming scheme available in Supporting Information.

peak arises at ~0.3 nm, a result in agreement with the results of Dahlberg et al. using quantum-mechanical methods for the CL headgroup.[50] The conformation of the headgroup was analyzed using the central O−C−C−C-O fragment represented by the $[\varphi_A/\varphi_B]$ torsional pair. In the 128TOCL and 128TMCL bilayers, the headgroup adopts an [−sc/−sc] conformation. This geometry allows hydrogen bonds to form between the hydroxyl oxygen and the phosphate oxygen atoms, in accordance with previous molecular simulations.[50] At the selected protonation state, with both acidic sites ionized, the secondary hydroxyl group of the CL headgroup is the only available source of hydrogen atoms to form inter- and intramolecular hydrogen bonds, which, in conjunction with the reduced mobility of the acyl chains and headgroup conformation help to explain the high second pK_a observed experimentally for CLs.[15]

3.1.3. Interaction of Cardiolipins with Ions. Cationic counterions, namely, 256 sodium ions, here, were added to the solvated system to ensure overall neutrality by compensating for the net negative charge of the CL bilayers, namely $2e^-$ per CL headgroup unit. On account of the high charged surface of the membrane and the high quantity of counterions introduced, use was made of a large layer of water to allow the latter to distribute better across the simulation cell. As has been mentioned previously and reported in Figure 2, the density of counterions overlaps with that of the lipid headgroups, specifically their phosphorus atoms. The present simulations indicate that not all the sodium ions interact directly with the CLs head groups. Only ~16% of the sodium atoms actually bind the carbonyl oxygen atoms in the first coordination shell, that is, within 0.33 nm, and about 30% were detected bound to the phosphate groups. About 68% of the counterions are not bound to CLs, the former participating in bridges between adjacent lipids through their phosphate or carbonyl groups. This observation is in agreement with previous molecular simulations carried out with different force fields, where both phosphate and carbonyl groups appear to be the primary sites for binding.[23,51]

3.1.4. Electrostatic Potential. To visualize how the electrostatic potential varies over the hydrated bilayer assay and analyze whether CLs could participate in the permeation of ionic solutes through the lipid bilayer, the average electrostatic potential of the 128TOCL system was mapped three-dimensionally using a PME-based approach (see Figure 5).[52]

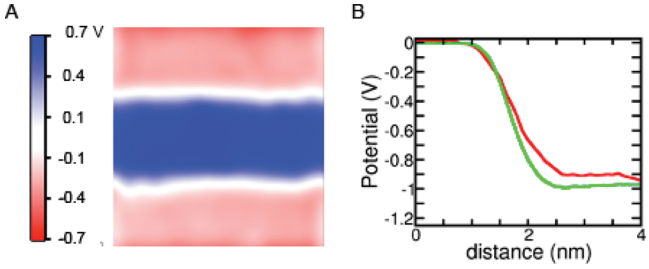

Figure 5. Electrostatic potential, Φ, of the hydrated CL bilayer. (A) Cross-section and (B) one-dimensional profile of the average electrostatic potential calculated with PME (red) and integration of charge density (green) along the normal to the pure TOCL membrane surface. (C).

Figure 4A shows a cross-section of this average in the *x*,*z*-plane. The computation of averaged electrostatic maps can be used subsequently to obtain a mean profile of the electrostatic potential in the direction normal to the plane of the bilayer (see Figure 5B). The latter profile reveals a surface potential at the locus of phosphorus atoms (~2.5 nm away from the center of the bilayer). This potential is about −30 mV when calculated as the difference between the values of the potential at the water midplane, a result in reasonable agreement with previous work.[23] This potential stems primarily from the interaction of the phosphate groups and the incomplete binding of counterions to the surface of the bilayer. A difference with a previous estimate based on the integration of the average charge distribution over the leaflets is detected for the membrane core potential. Here, the potential in the middle of the bilayer rises to about 0.8 V, when Dahlberg and Maliniak report a value of about 0.6 V.[23] To give support to the present results, the Poisson−Boltzmann equation was solved and averaged over 50 independent configurations of the bilayer assay (see Supporting Information), yielding a potential of 0.8 ± 0.2 V, which falls within our original estimate. The profile bears a noteworthy resemblance with the potential calculated using the PME approach, with a higher potential at the membrane core, when

dx.doi.org/10.1021/ct200849k | J. Chem. Theory Comput. 2012, 8, 1765−1773

compared with the POPG or POPC membrane potentials calculated from charge densities.[53] Aside from the debate on the best possible theoretical methods to determine electrostatic potentials, namely, integration of the charge distribution,[54] the particle-mesh Ewald summation method,[37] or the direct solution of the Poisson−Boltzmann equation, and the systematic overestimation of the membrane dipole potential when force fields that do not consider induction effects are employed,[55] the present results are suggestive of a barrier in the electrostatic potential that could markedly impede passive translocation of positive ions across the bilayer. This, in turn, could favor proton accumulation at the surface of the mitochondrial membrane. Haines and Dencher[10] put forth that CL head groups could participate in the creation of a proton gradient, which might serve as the inner mitochondrial membrane proton sink. Cherepanov et al.[56] have proposed a model where the negative charges of the inner mitochondrial membrane lipids retard proton equilibration between the membrane surface and the bulk, thereby supporting the formation of the proton motive force (PMF) required for ATPase function.

3.2. Mitochondrial Membrane Simulation. To explore further the range of applicability of the new parameters developed for CLs, a mixed-lipid bilayer (MIX) composed of POPE, POPG, and TMCL was simulated in order to mimic an inner mitochondrial membrane. Figure 6 depicts the

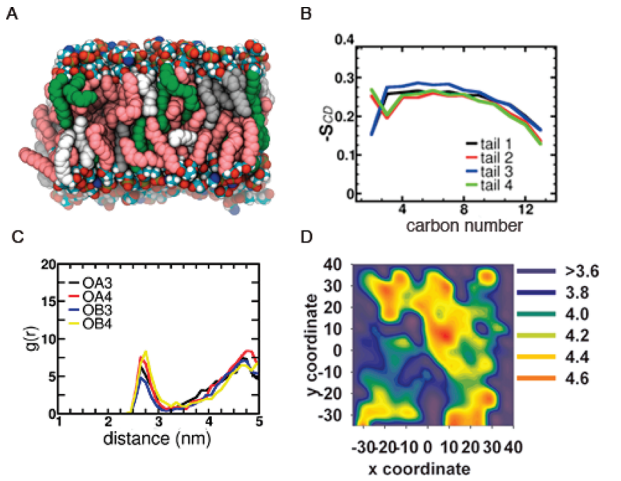

Figure 6. (A) Representative configuration of the mixed bilayer composed of POPE (pink) POPG (white, green) and TMCL (gray). (B) Local order parameter (S_{CD}) of the four acyl chains of TMCLs in presence of POPE:POPG lipids. (C) Intramolecular hydrogen bonds calculated using the pair correlation function between hydroxyl and phosphate oxygens. (D) Plot of the mixed bilayer thickness. Values calculated as phosphorus-to-phosphorus atom distance.

composition and properties of the MIX assay. The area per lipid for each component of the bilayer was calculated to appreciate how the presence of different lipids alters the behavior of the structure of the TMCLs. Instead of resorting to the canonical method described by Edholm and Nagle[57] to calculate A_L, the latter was calculated based on the contribution of each component to the total bilayer area, employing a Voronoi tessellation approach, as proposed by Shinoda and Okazaki.[38] In Figure 7, a representative snapshot of the bilayer is provided, alongside with a superimposition of the Voronoi polygons of it, calculated using the projection onto the *x*,*y*-plane of the center of mass of each lipid molecule in a given

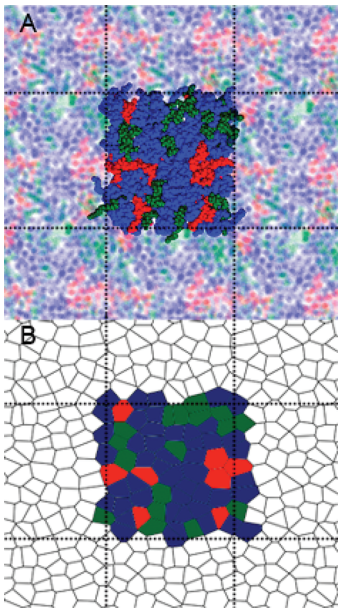

Figure 7. (A) Representative POPE/POPG/TMCL bilayer. (B) Voronoi tessellation of the membrane lipids: TMCL (red), POPG (green), and POPE (blue). Dot lines represent periodic cell boundaries.

leaflet. Because CL is an extended lipid, which can be described in terms of two lipids joined by a single glycerol moiety, the equivalent area per phosphate group $\langle Ae_L \rangle$ was also calculated.

As may be observed in Table 2, TMCLs in the mixed-lipid membrane exhibit a lower A_L − namely about 1.4 times, with

Table 2. Area Per Lipid of POPE/POPG/TMCL Mixed−Lipid Membrane

	TMCL	POPG	POPE
% total area	0.13	0.21	0.65
$\langle A_L \rangle$ nm^2	0.71 ± 0.1	0.62 ± 0.1	0.60 ± 0.1
$\langle Ae_L \rangle$ nm^2	0.43 ± 0.3		

respect to the pure bilayer simulation, a result also confirmed by the use of the Ae_L, for which a decrease of 1.3 times is observed. This compression of TMCLs is compensated by the increase of A_L for POPE compared with the values obtained from simulations of pure bilayers with the same headgroup force field.[26] Direct assessment of the change of A_L for POPG is not possible on account of the absence of experimental information or simulation of pure bilayers with the c36 force field. The presence of different kinds of lipids reduce the ordering of the acyl chains when compared with the simulation of pure lipid bilayers for TMCL (Figure 6B), with the same effect observed on simulations of mixed lipid bilayers containing POPE and POPG. The headgroup in TMCL adopts both [−sc/−sc] and [−sc/ap] conformations. These headgroup conformations allow intramolecular hydrogen bonds to form, as described for the pure bilayers (Figure 6C). Beyond the force field or the simulation protocols, the observed differences in A_L, S_{CD}, and headgroup conformation are suggestive of an effect of CL on the mechanical properties of the mixed bilayer. Variations of the membrane thickness (Figure 6D), and differences in the area per lipid of TMCL, POPE, and POPG result in a nonuniform surface of the membrane and a variety of interactions with counterions or

other lipids. This nonuniformity of the surface of CL-containing bilayers could help optimize the interaction of the membrane with proteins, where CLs participate as a scaffold tethering the membrane protein, or possibly decrease the fluidity of the bilayer in a similar manner as does cholesterol in eukaryotic membranes.[58,59] As an example, larger quantities of CL (about 55−60 mol %) can be found in some microbial organisms, where the ordered CL chains enhance the structural integrity of the cell membrane, allowing the organism to resist stress conditions.[60] Acehan et al. hypothesized a participation of CLs in the promotion of the ribbon-like assembly of ATP synthase dimers, where the presence of CLs affects the lateral organization and morphology of the membrane.[61]

The hybrid all-atom/united-atom force-field parameters for CLs reported here imply a ca. 50% reduction in the number of lipid atoms, hence allowing noticeably larger bilayer patches to be simulated with a reduced computational cost. The appreciable reduction of the number of atoms is anticipated to help in studies where CLs are hypothesized to contribute to the mechanical properties of mitochondrial membranes, and for which sizable assays and lengthy simulations are required to account for undulations of large amplitude.[62] Furthermore, the strategy developed here can be extended seamlessly to other CLs, which might be required for the investigation of other lipid bilayers composed of CLs with different acyl chains.

4. CONCLUSIONS

In this contribution, a new set of parameters for cardiolipins (TOCL and TMCL) is developed in the framework of the c36 force field and designed with the ultimate objective to perform simulations of cardiolipin-containing mixed-lipid membranes, chief among which are mitochondrial membranes. In the absence of experimental data, the simulations of pure CL bilayers described herein have been compared with previously published theoretical investigations. Our results for pure TOCL and TMCL bilayers are in good agreement with observables from other simulations, such as the area per lipid and the thickness, although discrepancies in the compressibility and the order parameter of the bilayers can be found. Altogether, these observables describe a possible metastable state of the CL bilayer, which is near the L_α/L_β phase transition temperature. Simulation of a mixed bilayer containing CLs provides valuable insight into the role played by CLs in the structure of the mitochondrial membrane, where they are envisioned to participate in the ordering of the acyl chains and to thickening of the membrane: properties related to the mitochondrial membrane characteristics and activity. The use of the united atom parameters c27-UA in conjunction with the all-atom c36 force field has proven to constitute a reasonable strategy to reduce the computational cost of membrane simulations without loss of accuracy. Additional simulations using this hybrid all-atom/united-atom force-field approximation are currently underway, exploring bigger bilayers composed of CLs and lipid mixtures aimed at achieving a better representation of mitochondrial membranes.

■ ASSOCIATED CONTENT

Supporting Information

The topology and parameter files for cardiolipins. This material is available free of charge via the Internet at http://pubs.acs.org.

■ AUTHOR INFORMATION

Corresponding Author

*E-mail: chipot@ks.uiuc.edu.

Notes

The authors declare no competing financial interest.

■ ACKNOWLEDGMENTS

We thank to Paz Tapia for technical support. D.A. thank to "Programa de Doctorado en Ciencias Aplicadas" from Universidad de Talca, Chile for financial support. The "Centro Interdisciplinario de Neurociencia de Valparaíso" is a Millennium Science Institute. The CONICYT is gratefully acknowledged for the funding of a visiting scholar position.

■ REFERENCES

(1) Zambrano, F.; Fleischer, S.; Fleischer, B. Lipid composition of the golgi apparatus of rat kidney and liver in comparison with other subcellular organelles. *Biochim. Biophys. Acta, Lipids Lipid Metab.* **1975**, *380*, 357−369.

(2) Jiang, F.; Ryan, M.; Schlame, M.; Zhao, M.; Gu, Z.; Klingenberg, M.; Pfanner, N.; Greenberg, M. Absence of cardiolipin in the crd1 null mutant results in decreased mitochondrial membrane potential and reduced mitochondrial function. *J. Biol. Chem.* **2000**, *275*, 22387−22394.

(3) Hoch, F. L. Minireview: Cardiolipins and mitochondrial proton-selective leakage. *J. Bioenerg. Biomembr.* **1998**, *30*, 511−532.

(4) Pember, S. O.; Powell, G. L.; Lambeth, J. D. Cytochrome P-450scc-phospholipid interactions. Evidence for a cardiolipin binding site and thermodynamics of enzyme interactions with cardiolipin, cholesterol, and adrenodoxin. *J. Biol. Chem.* **1983**, *258*, 3198−3206.

(5) Müller, M.; Moser, R.; Cheneval, D.; Carafoli, E. Cardiolipin is the membrane receptor for mitochondrial creatine phosphokinase. *J. Biol. Chem.* **1985**, *260*, 3839−3843.

(6) Schlattner, U.; Wallimann, T. A Quantitative approach to membrane binding of human ubiquitous mitochondrial creatine kinase using surface plasmon resonance. *J. Bioenerg. Biomembr.* **2000**, *32*, 123−131.

(7) Beleznai, Z.; Jancsik, V. Role of cardiolipin in the functioning of mitochonbrial L-glycerol-3-phosphate dehydrogenase. *Biochem. Biophys. Res. Commun.* **1989**, *159*, 132−139.

(8) Noël, H.; Pande, S. V. An essential requirement of cardiolipin for mitochondrial carnitine acylcarnitine translocase activity. *Eur. J. Biochem.* **1986**, *155*, 99−102.

(9) Gonzalvez, F.; Gottlieb, E. Cardiolipin: setting the beat of apoptosis. *Apoptosis* **2007**, *12*, 877−885.

(10) Haines, T. H.; Dencher, N. A. Cardiolipin: A proton trap for oxidative phosphorylation. *FEBS Lett.* **2002**, *528*, 35−39.

(11) Ott, M.; Robertson, J. D.; Gogvadze, V.; Zhivotovsky, B.; Orrenius, S. Cytochrome c release from mitochondria proceeds by a two-step process. *Proc. Natl. Acad. Sci. U.S.A.* **2002**, *99*, 1259−1263.

(12) Ardail, D.; Privat, J. P.; Egret-Charlier, M.; Levrat, C.; Lerme, F.; Louisot, P. Mitochondrial contact sites. Lipid composition and dynamics. *J. Biol. Chem.* **1990**, *265*, 18797−18802.

(13) Huang, K. C.; Mukhopadhyay, R.; Wingreen, N. S. A Curvature-Mediated Mechanism for Localization of Lipids to Bacterial Poles. *PLoS Comput. Biol.* **2006**, *2*, No. e151, DOI: 10.1371/journal.-pcbi.0020151.

(14) Winterhalter, M.; Van Gelder, P.; Dumas, F. Understanding the function of bacterial outer membrane channels by reconstitution into black lipid membranes. *Biophys. Chem.* **2000**, *85*, 153−167.

(15) Lewis, R. N. A. H.; McElhaney, R. N. The physicochemical properties of cardiolipin bilayers and cardiolipin-containing lipid membranes. *Biochim. Biophys. Acta, Biomembr.* **2009**, *1788*, 2069−2079.

(16) McAuley, K. E.; Fyfe, P. K.; Ridge, J. P.; Isaacs, N. W.; Cogdell, R. J.; Jones, M. R. Structural details of an interaction between

cardiolipin and an integral membrane protein. *Proc. Natl. Acad. Sci. U.S.A.* **1999**, *96*, 14706−14711.
(17) Camara-Artigas, A.; Magee, C. L.; Williams, J. C.; Allen, J. P. Individual interactions influence the crystalline order for membrane proteins. *Acta Crystallogr., Sect. D: Biol. Crystallogr.* **2001**, *57*, 1281−1286.
(18) Roszak, A. W.; Gardiner, A. T.; Isaacs, N. W.; Cogdell, R. J. Brominated lipids identify lipid binding sites on the surface of the reaction center from Rhodobacter sphaeroides. *Biochemistry* **2007**, *46*, 2909−2916.
(19) Tsukihara, T.; Shimokata, K.; Katayama, Y.; Shimada, H.; Muramoto, K.; Aoyama, H.; Mochizuki, M.; Shinzawa-Itoh, K.; Yamashita, E.; Yao, M.; Ishimura, Y.; Yoshikawa, S. The low-spin heme of cytochrome c oxidase as the driving element of the proton-pumping process. *Proc. Natl. Acad. Sci. U.S.A.* **2003**, *100*, 15304−15309.
(20) Marrink, S. J.; de Vries, A. H.; Tieleman, D. P. Lipids on the move: Simulations of membrane pores, domains, stalks and curves. *Biochim. Biophys. Acta, Biomembr.* **2009**, *1788*, 149−168.
(21) Chipot, C.; Klein, M. L.; Tarek, M. Modeling lipid membranes. *Handbook of Materials Modeling*: Springer: Netherlands, 2005, 929−958.
(22) Dahlberg, M. Polymorphic phase behavior of cardiolipin derivatives studied by coarse-grained molecular dynamics. *J. Phys. Chem. B* **2007**, *111*, 7194−7200.
(23) Dahlberg, M.; Maliniak, A. Molecular dynamics simulations of cardiolipin bilayers. *J. Phys. Chem. B* **2008**, *112*, 11655−11663.
(24) Berger, O.; Edholm, O.; J hnig, F. Molecular dynamics simulations of a fluid bilayer of dipalmitoylphosphatidylcholine at full hydration, constant pressure, and constant temperature. *Biophys. J.* **1997**, *72*, 2002−2013.
(25) Róg, T.; Martinez-Seara, H.; Munck, N.; Oresic, M.; Karttunen, M.; Vattulainen, I. Role of cardiolipins in the inner mitochondrial membrane: insight gained through atom-scale simulations. *J. Phys. Chem. B* **2009**, *113*, 3413−3422.
(26) Klauda, J. B.; Venable, R. M.; Freites, J. A.; O'Connor, J. W.; Tobias, D. J.; Mondragon-Ramirez, C.; Vorobyov, I.; MacKerell, A. D.; Pastor, R. W. Update of the CHARMM all-atom additive force field for lipids: Validation on six lipid types. *J. Phys. Chem. B* **2010**, *114*, 7830−7843.
(27) Hénin, J.; Shinoda, W.; Klein, M. L. Models for phosphatidylglycerol lipids put to a structural test. *J. Phys. Chem. B* **2009**, *113*, 6958−6963.
(28) Hénin, J.; Shinoda, W.; Klein, M. L. United-atom acyl chains for CHARMM phospholipids. *J. Phys. Chem. B* **2008**, *112*, 7008−7015.
(29) *Hyperchem*, release 7.0;, Hypercube, Inc.: Gainesville, FL, 2002.
(30) Stewart, J. J. P. Optimization of parameters for semiempirical methods I. Method. *J. Comput. Chem.* **1989**, *10*, 209−220.
(31) Humphrey, W.; Dalke, A.; Schulten, K. VMD: Visual molecular dynamics. *J. Mol. Graphics* **1996**, *14*, 33−38.
(32) Phillips, J.; Braun, R.; Wang, W.; Gumbart, J.; Tajkhorshid, E.; Villa, E.; Chipot, C.; Skeel, R.; Kale, L.; Schulten, K. Scalable molecular dynamics with NAMD. *J. Comput. Chem.* **2005**, *26*, 1781−1802.
(33) Feller, S. E.; Zhang, Y. H.; Pastor, R. W.; Brooks, B. R. Constant-pressure molecular-dynamics simulation—The Langevin piston method. *J. Chem. Phys.* **1995**, *103*, 4613−4621.
(34) Tuckerman, M. E.; Berne, B. J.; Rossi, A. Molecular dynamics algorithm for multiple time scales: Systems with disparate masses. *J. Chem. Phys.* **1991**, *94*, 1465−1469.
(35) Jorgensen, W.; Chandrasekhar, J. M.; Jd, I. RW; Klein, M. L. Comparison of simple potential functions for simulating liquid water. *J. Chem. Phys.* **1983**, *79*, 926−935.
(36) MacKerell, A. D.; Bashford, D.; Bellott; Dunbrack, R. L.; Evanseck, J. D.; Field, M. J.; Fischer, S.; Gao, J.; Guo, H.; Ha, S.; Joseph-McCarthy, D.; Kuchnir, L.; Kuczera, K.; Lau, F. T. K.; Mattos, C.; Michnick, S.; Ngo, T.; Nguyen, D. T.; Prodhom, B.; Reiher, W. E.; Roux, B.; Schlenkrich, M.; Smith, J. C.; Stote, R.; Straub, J.; Watanabe, M.; Wirkiewicz-Kuczera, J.; Yin, D.; Karplus, M. All-atom empirical potential for molecular modeling and dynamics studies of proteins. *J. Phys. Chem. B* **1998**, *102*, 3586−3616.
(37) Aksimentiev, A.; Schulten, K. Imaging [alpha]-hemolysin with molecular dynamics: ionic conductance, osmotic permeability, and the electrostatic potential map. *Biophys. J.* **2005**, *88*, 3745−3761.
(38) Okazaki, S.; Shinoda, W. A Voronoi analysis of lipid area fluctuation in a bilayer. *J. Chem. Phys.* **1998**, *109*, 1517−1521.
(39) Janosi, L.; Gorfe, A. A. Simulating POPC and POPC/POPG bilayers: conserved packing and altered surface reactivity. *J. Chem. Theory Comput.* **2010**, *6*, 3267−3273.
(40) Pastor, R. W.; MacKerell, A. D. Development of the CHARMM force field for lipids. *J. Phys. Chem. Lett.* **2011**, *2*, 1526−1532.
(41) Goormaghtigh, E.; Ruysschaert, J. M. Role of the cardiolipin-adriamycin complex in mitochondrial toxicity. *Colloids Surf.* **1984**, *10*, 239−247.
(42) Goormaghtigh, E.; Huart, P.; Praet, M.; Brasseur, R.; Ruysschaert, J. M. Structure of the adriamycin-cardiolipin complex: Role in mitochondrial toxicity. *Biophys. Chem.* **1990**, *35*, 247−257.
(43) Zhao, W.; Róg, T.; Gurtovenko, A.; Vattulainen, I.; Karttunen, M. Atomic-scale structure and electrostatics of anionic palmitoyloleoylphosphatidylglycerol lipid bilayers with Na+ counterions. *Biophys. J.* **2007**, *92*, 1114−1124.
(44) Elmore, D. E. Molecular dynamics simulation of a phosphatidylglycerol membrane. *FEBS Lett.* **2006**, *580*, 144−148.
(45) Petrache, H. I.; Tristram-Nagle, S.; Gawrisch, K.; Harries, D.; Parsegian, V. A.; Nagle, J. F. Structure and fluctuations of charged phosphatidylserine bilayers in the absence of salt. *Biophys. J.* **2004**, *86*, 1574−1586.
(46) Ulmschneider, J. P.; Ulmschneider, M. B. United atom lipid parameters for combination with the optimized potentials for liquid simulations all-atom force field. *J. Chem. Theory Comput.* **2009**, *5*, 1803−1813.
(47) Wang, Y.; Ohkubo, Y.; Tajkhorshid, E. Gas conduction of lipid bilayers and membrane channels. In *Computational Modeling of Membrane Bilayers*; Feller, S., Ed.; Current Topics in Membranes; Elsevier, 2008; Vol. *60*, pp 343−367.
(48) Lewis, R. N. A. H.; Zweytick, D.; Pabst, G.; Lohner, K.; McElhaney, R. N. Calorimetric, X-ray diffraction, and spectroscopic studies of the thermotropic phase behavior and organization of tetramyristoyl cardiolipin membranes. *Biophys. J.* **2007**, *92*, 3166−3177.
(49) Marrink, S. J.; de Vries, A. H.; Mark, A. E. Coarse grained model for semiquantitative lipid simulations. *J. Phys. Chem. B* **2004**, *108*, 750−760.
(50) Dahlberg, M.; Marini, A.; Mennucci, B.; Maliniak, A. Quantum chemical modeling of the cardiolipin headgroup. *J. Phys. Chem. A* **2010**, *114*, 4375−4387.
(51) Pöyry, S.; Róg, T.; Karttunen, M.; Vattulainen, I. Mitochondrial membranes with mono- and divalent salt: Changes induced by salt ions on structure and dynamics. *J. Phys. Chem. B* **2009**, *113*, 15513−15521.
(52) Batcho, P. F.; Case, D. A.; Schlick, T. Optimized particle-mesh Ewald/multiple-time step integration for molecular dynamics simulations. *J. Chem. Phys.* **2001**, *115*, 4003.
(53) Zhao, W.; Róg, T.; Gurtovenko, A.; Vattulainen, I.; Karttunen, M. Role of phosphatidylglycerols in the stability of bacterial membranes. *Biochimie* **2008**, *90*, 930−938.
(54) Lamoureux, G.; Harder, E.; Vorobyov, I. V.; Roux, B.; Mackerell, A. D., Jr. A polarizable model of water for molecular dynamics simulations of biomolecules. *Chem. Phys. Lett.* **2006**, *418*, 245−249.
(55) Baker, C. M.; Lopes, P. E. M.; Zhu, X.; Roux, B.; Mackerell, A. D., Jr. Accurate calculation of hydration free energies using pair-specific Lennard-Jones parameters in the CHARMM drude polarizable force field. *J. Chem. Theory Comput.* **2010**, *6*, 1181−1198.
(56) Cherepanov, D. A.; Feniouk, B. A.; Junge, W.; Mulkidjanian, A. Y. Low dielectric permittivity of water at the membrane interface: effect on the energy coupling mechanism in biological membranes. *Biophys. J.* **2003**, *85*, 1307−1316.

(57) Edholm, O.; Nagle, J. F. Areas of molecules in membranes consisting of mixtures. *Biophys. J.* **2005**, *89*, 1827−1832.
(58) Epand, R. M.; Epand, R. F. Lipid domains in bacterial membranes and the action of antimicrobial agents. *Biochim. Biophys. Acta* **2009**, *1788*, 289−294.
(59) Kaiser, H.-J.; Surma, M. A.; Mayer, F.; Levental, I.; Grzybek, M.; Klemm, R. W.; Da Cruz, S.; Meisinger, C.; Muller, V.; Simons, K.; Lingwood, D. Molecular convergence of bacterial and eukaryotic surface order. *J. Biol. Chem.* **2011**, *286*, 40631−40637.
(60) Hoch, F. L. Cardiolipins and biomembrane function. *Biochim. Biophys. Acta* **1992**, *1113*, 71−133.
(61) Acehan, D.; Malhotra, A.; Xu, Y.; Ren, M.; Stokes, D. L.; Schlame, M. Cardiolipin affects the supramolecular organization of ATP synthase in mitochondria. *Biophys. J.* **2011**, *100*, 2184−2192.
(62) Sachs, J. N.; Braun, A. R.; Brandt, E. G.; Edholm, O.; Nagle, J. F. Determination of electron density profiles and area from simulations of undulating membranes. *Biophys. J.* **2011**, *100*, 2112−2120.